Influence of manufacturing tolerances and eccentricities on the unbalanced magnetic pull in permanent magnet synchronous motors

Unai Galfarsoro, Alex McCloskey, Sergio Zarate, Xabier Hernández, Gaizka Almandoz, Member, IEEE

Abstract – Eccentricity is an inevitable fault in electric motors and hence its diagnosis is an important topic. Thus, the influence of static and dynamic eccentricities on the harmonics of the frequency spectra of the unbalanced magnetic pull is analyzed.

In this study, dimensional tolerances of the rotor and the stator are also considered. All parts have dimensional tolerances in their designs and their real magnitudes vary to some extent from the theoretical values after the manufacturing process. Thanks to analytical calculations and finite element simulations, verified with experimental results, it is observed that the deviations originated by the manufacturing tolerances produce changes in the amplitudes of some harmonics and also additional and characteristic harmonics in the frequency spectra of the unbalanced magnetic pull. These are not negligible and must be taken into account when robust eccentricity detection procedures are defined. Otherwise, harmonics originated by tolerances and by eccentricities can be misidentified.

Finally, after decoupling the effect of tolerances and eccentricities, the frequency harmonics that are indicators of rotor tolerances are determined, and a new methodology based on ratios of amplitudes of adjacent harmonics is proposed to identify eccentricities.

Index Terms -- Fault detection, Fault diagnosis, Force measurement, Permanent magnet machines, Tolerance analysis.

I. INTRODUCTION

The use of electric motors (EMs) is widespread, and is probably going to increase due to the ongoing success of electric vehicles [1]. Yilmaz [2] states that the main kinds of EMs for plug-in hybrid electric vehicles are induction motors (IMs), permanent magnet synchronous motors (PMSMs), DC motors and switched reluctance motors. IMs and PMSMs are winning importance, and PMSMs are leaders in the market. Yilmaz [2] and Riba et al. [3] remark that PMSMs, compared to IMs, are less reliable and technologically mature.

Therefore, since PMSMs are a mass-produced product with a non-negligible danger of failure, it is justified to research the effect of their design on their reliability. According to Hong et al. [4], bearing faults, eccentricities and demagnetization of the permanent magnets (PMs) are the major causes of failures in PMSMs.

This paper analyzes the effect of static eccentricity (SE) and dynamic eccentricity (DE) by analytical methods, simulation and experimental measurements. In a healthy and ideal EM, the rotation axis of the rotor (O_W) is the same as its symmetry axis (O_r), and both match with the symmetry axis of the stator bore (O_S) (see Fig. 1). In this case the air-gap around the rotor is uniform and time independent. With SE the rotation axis of the rotor coincides with its symmetry axis, but it is shifted with respect to the symmetry axis of the stator bore. Therefore, the air-gap around the rotor is not uniform but it is time independent, that is, the zones of minimum and maximum air-gap are always placed on the same location. With DE the rotation axis of the rotor coincides with the symmetry axis of the stator bore but it does not coincide with its symmetry axis. Again the air-gap around the rotor is not uniform, but now it is time dependent because the minimum air-gap position rotates with the rotor. Mixed eccentricity (ME) is the sum of SE and DE. The results for ME can be assumed to be the sum of the results of SE and DE. Eccentricity is a crucial defect that generates further magnetic and dynamic problems, torque ripple and unbalanced magnetic pull (UMP) [5], triggering additional vibrations and noise [6]. UMP is a radial force that remains fixed in space for SE and rotates with the rotor for DE [5][7]. Without eccentricity (WE) there would be no UMP. Hong et al. [4], Nandi et al. [8] and Ebrahimi et al. [9] declare that the lowest eccentricity value to take into account is about 5-10% of the air gap. Manufacturing and installation of the EMs create acceptable inherent eccentricity levels below 5-10%.

$$O_S = O_r = O_w \qquad O_S \qquad O_r = O_w \qquad O_S = O_w \qquad O_r$$
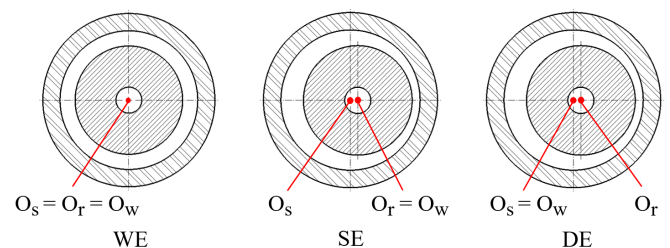WE　　　　　　SE　　　　　　DE

Fig. 1. Geometric explanation of eccentricity cases: without eccentricity (WE), static eccentricity (SE) and dynamic eccentricity (DE)

The originality of this study is that dimensional tolerances of the rotor and the stator are considered, analyzing these cases: without tolerances (WT), rotor tolerances (RT), stator tolerances (ST) and both tolerances (BT). All pieces have dimensional tolerances in their designs and their real magnitudes vary to some extend from the theoretical values after the manufacturing process. Fig. 2 is an example of a PMSM with dimensions in the rotor and the stator that vary from the theoretical ones. This dimensional irregularities cause changes in the UMP of PMSMs, which may not be negligible compared to those that arise due to eccentricities, and thus have to be separated from the fault indicators to detect SE and DE.

Fig. 2. Example of PMSM with rotor tolerances and stator tolerances

Bramerdorfer [13] carried out tolerance analysis for EM design optimization by statistical calculations, and observed the cogging torque and back-EMF sensitivity of an interior PMSM regarding changes in the material characteristics. The results clearly indicate that the tolerance analysis is essential for the design of the machine.

Taran et al. [14] studied three PM EMs with different configurations for dimensional and material tolerances, by FE simulation and by experimental measurements. A tolerance of ± 0.1 mm, considered typical for laser cutting prototyping, is considered for eleven geometrical input design variables. Additionally, a ± 5% is considered for the PM remanence in order to account for possible variations both in the material grade and in the external magnetization. The effect of SE on the amplitude of the time signal of the back-EMF and cogging torque of an axial flux PM motor is analyzed. The conclusion is that variations in time signals are too small to have a sensitive enough method, and further studies based on frequency harmonics and side bands are suggested.

According to [14], a systematic study of dimensional and material tolerances is of the utmost importance in the process of designing and manufacturing an EM.

However, no papers that study the influence of eccentricity and manufacturing tolerances of the rotor and the stator on the UMP of PMSMs were found.

The contributions of this article are:
1. Demonstration of the combined effect of eccentricities and manufacturing tolerances in the frequency spectrum of the UMP.
2. Calculation of the frequencies that arise in the spectrum of the UMP depending on eccentricity type (WE, SE or DE) and/or tolerance type (WT, RT, ST and BT). This is determined for the magnitude of the UMP and for the projection of the UMP in a fixed direction.
3. A methodology to detect frequencies that are indicators of RT, and independent of eccentricity.
4. A methodology to detect frequencies that are indicators of each type of eccentricity (SE or/and DE), and independent of manufacturing tolerances.

This knowledge is important for the design stage of EMs to minimize the harmful effects of UMP in their performance (with more vibrations) and durability (with reduced bearings life), assessing the disturbing influence of the manufacturing tolerances.

II. ANALYTICAL CALCULATIONS

Analytical calculations are carried out to have an insight of the frequency orders generated in the UMP, for the PMSM operating under various eccentricity and tolerance types. It is important to remark that the amplitudes of the harmonics of the UMP are of no interest in this study, only the frequency content (as mechanical orders) is sought.

WE, SE and DE eccentricities, and/or RT and ST are included in this assessment. Frequency orders are calculated in the presence or not of these eccentricities and tolerances, without studying different eccentricity amplitudes nor tolerance profiles and amplitudes. When RT or ST are taken into account, the presence of any generic deviation in amplitude, width, etc. with regard to the theoretical configurations is considered as a whole. Any of these "global" deviations generates characteristic orders in the frequency domain spectra, allowing to associate the changes in the orders to a RT and/or a ST, and/or to a SE and/or a DE.

A. Without eccentricity

The magnetic pressure generates a resultant net force, named the UMP, on the surface of the rotor and the stator in the direction of the shortest air gap. The UMP must be minimized because it can trigger negative effects like vibrations, instability, wear in bearings, etc.

From the magnetic flux density, and using the Maxwell stress tensor, the electromagnetic pressure is calculated. The magnetic flux density is mainly radial and its tangential component is negligible compared to the radial one, and hence, the radial magnetic pressure is calculated according to [15][16][17][18][19][20][21]:

$$p_r(\theta, t) \approx \frac{\left(B_r(\theta, t)\right)^2}{2\mu_0} \tag{1}$$

being p_r the radial magnetic pressure, B_r the radial magnetic flux density, μ_0 the magnetic permeability of the air. Both the radial magnetic pressure and the radial magnetic flux density vary with the time t and the tangential position θ.

Analytical calculations of the UMP for fractional PM machines were carried out by [22][23], including the analysis of the influence of the combinations of the numbers of pole pairs and slots (hereinafter p and Qs respectively). The horizontal UMP_x and the vertical UMP_y components of the resultant net force (the UMP) on the rotor are calculated integrating the projections of the force in the horizontal and the vertical directions in a whole turn [22][23]:

$$UMP_x = L_{stk} R_{rot} \int_0^{2\pi} \frac{\left(B_r(\theta, t)\right)^2}{2\mu_0} \cos\theta \, d\theta$$

$$UMP_y = L_{stk} R_{rot} \int_0^{2\pi} \frac{\left(B_r(\theta, t)\right)^2}{2\mu_0} \sin\theta \, d\theta \tag{2}$$

where L_{stk} and R_{rot} are the total axial length of the rotor (that is, the total axial length of the magnets) and the radius of the metal sheet stacks of the rotor respectively. The tangential

position θ is referenced to the horizontal orientation.

The squared magnetic flux density can be calculated first without the influence of the slots of the stator, and then it can be updated with the influence of these slots in the following way:

$$\left(B_r(\theta,t)\right)^2 = \left(B_r^m(\theta,t)\right)^2 \lambda(\theta) \tag{3}$$

being $B_r(\theta,t)$ the magnetic flux density, $B_r^m(\theta,t)$ the magnetic flux density generated by the magnets only (without the slots) and $\lambda(\theta)$ the slots function. Fig. 3 shows all these variables for half a turn of the rotor.

The squared magnetic flux density generated by the magnets only (that is, without the slots), $\left(B_r^m(\theta,t)\right)^2$, is generally represented by a Fourier series [18][24]:

$$\left(B_r^m(\theta,t)\right)^2 = \sum_{k=1}^{\infty} B_{r\,k}^{m2} \cos(2\pi f_{rot} k\,t - k\theta) \tag{4}$$

being $B_{r\,k}^{m2}$ and k the coefficients and the harmonic's order of the Fourier series respectively, and f_{rot} the rotational speed of the rotor in Hz.

Since the squared magnetic flux density generated by the magnets only, $\left(B_r^m(\theta,t)\right)^2$, has a period of $2\pi/2p$, as shown in Fig. 3 b), the harmonics of the squared magnetic flux density of the magnets, k, will be multiples of $2p$ (see (5)). But that is the case if all the magnets are equal and are located equispaced in the rotor. Otherwise, if due to the effect of tolerances the rotor is magnetically non symmetric and is not balanced in all the turn, the period is 2π and the harmonics k can take any integer value 0, 1, 2, 3…, $2p$, $4p$, $6p$… (see (6)).

Without rotor tolerances: $k = 0, 2p, 4p, 6p ... = u(2p)$ (5)

With rotor tolerances: $k = 0,1,2,3... 2p, 4p, 6p ...$ (6)

being $u = 0,1,2,3…$ an integer number.

The slots function, $\lambda(\theta)$, is also represented by a Fourier series:

$$\lambda(\theta) = \sum_{\ell=0}^{\infty} \lambda_\ell \cos(\ell\theta) \tag{7}$$

Since the slots function, $\lambda(\theta)$, has a period of $2\pi/Q_s$, as shown in Fig. 3 c), the harmonics of the slots function, ℓ, will be multiples of Q_s if the stator is ideal (see (8)). Furthermore, if due to the effect of tolerances the stator is non-ideal, the period is 2π, and these harmonics ℓ can take any integer value 0,1,2,3…, Q_s, $2Q_s$, $3Q_s$… (see (9)).

Without stator tolerances: $\ell = 0, Q_s, 2Q_s, 3Q_s ... = vQ_s$ (8)

With stator tolerances: $\ell = 0,1,2,3... Q_s, 2Q_s, 3Q_s ...$ (9)
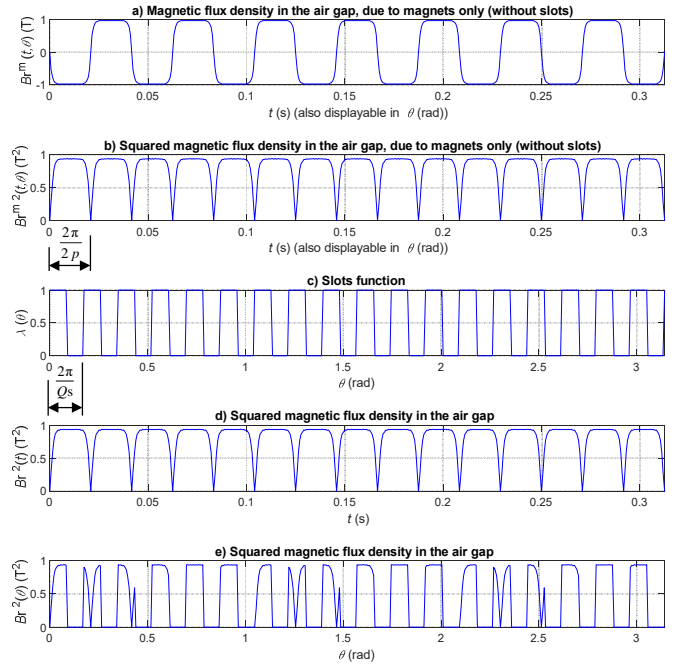
being $v = 0,1,2,3…$ an integer number.

Fig. 3. a) Magnetic flux density by the magnets only, $B_r^m(\theta,t)$; b) Squared magnetic flux density generated by the magnets only, $\left(B_r^m(\theta,t)\right)^2$; c) The slots function $\lambda(\theta)$; d) Squared magnetic flux density in time domain, $\left(B_r(t)\right)^2$; e) Squared magnetic flux density in tangential position domain, $\left(B_r(\theta)\right)^2$

Introducing equations (4) and (7) into (3):

$$\left(B_r(\theta,t)\right)^2 = \sum_{k=1}^{\infty}\sum_{\ell=0}^{\infty} \frac{B_{r\,k}^{m2}\lambda_\ell}{2}\Big[\cos\big(2\pi f_{rot}k\,t-(k+\ell)\theta\big)+ \\ + \cos\big(2\pi f_{rot}k\,t-(k-\ell)\theta\big)\Big] \tag{10}$$

Next, the horizontal component UMP_x of the net force is developed from (2):

$$UMP_x = \frac{L_{stk}R_{rot}}{2\mu_0}\int_0^{2\pi}\sum_{k=1}^{\infty}\sum_{\ell=0}^{\infty}\frac{B_{r\,k}^{m2}\lambda_\ell}{2}\Big[\cos\big(2\pi f_{rot}k\,t-(k+\ell)\theta\big)+ \\ + \cos\big(2\pi f_{rot}k\,t-(k-\ell)\theta\big)\Big]\cos\theta\,d\theta = \\ = \frac{L_{stk}R_{rot}}{2\mu_0}\int_0^{2\pi}\sum_{k=1}^{\infty}\sum_{\ell=0}^{\infty}\frac{B_{r\,k}^{m2}\lambda_\ell}{4}\Big[\cos\big(2\pi f_{rot}k\,t-(k+\ell+1)\theta\big)+ \\ + \cos\big(2\pi f_{rot}k\,t-(k+\ell-1)\theta\big)+\cos\big(2\pi f_{rot}k\,t-(k-\ell+1)\theta\big)+ \\ + \cos\big(2\pi f_{rot}k\,t-(k-\ell-1)\theta\big)\Big]d\theta \tag{11}$$

To have non-zero values of UMP_x, any of the four conditions of (12) obtained from the spatial distribution order of the magnetic pressure must be fulfilled. These conditions can be summarized as (13).

$$\begin{aligned} k+\ell+1=0 && k+\ell-1=0 \\ k-\ell+1=0 && k-\ell-1=0 \end{aligned} \tag{12}$$

$$k \pm \ell = \pm 1 \tag{13}$$

Result (13), for a non-tolerance case, is the same as the condition obtained by [17][19][22]. Thus, if the spatial frequency of a magnetic pressure wave is ±1 the resultant

UMP_x is not zero. Huo et al. [24] conclude that the UMP is created when $u \cdot 2p \pm v \cdot Q\mathrm{s} = \pm 1$, where u and v are integers that correspond to the harmonics of the magneto magnemotive force of the magnets and the slots. These results agree with (13).

In the case of an ideal PMSM with no tolerances, from (5) and (8) the harmonics of the squared magnetic flux density are when $k = u(2p)$ and the harmonics of the slots $\ell = vQ\mathrm{s}$, so the next condition must be fulfilled to induce a non-zero UMP_x:

$$u(2p) \pm vQ\mathrm{s} = \pm 1 \tag{14}$$

$k = u(2p)$ harmonics matching this condition need to be considered.

If tolerances are taken into account in the PMSM, from (6) and (9) the harmonics k of the squared magnetic flux density and the harmonics ℓ of the slots can contain any value, so any of the conditions of (15) must be fulfilled to induce a non-zero UMP_x. This means that many combinations are possible and that all the harmonics of the squared magnetic flux density k will appear.

$$
\begin{array}{ccccc}
k = 0 & k = 1 & k = 2 & k = 1 & k = 3 \\
\ell = 1 & \ell = 0 & \ell = 1 & \ell = 2 & \ell = 2
\end{array} \quad \text{etc.} \tag{15}
$$

If the tolerances of the magnets are predominant, the stator can be considered perfect and then from (8) the slot harmonics are $\ell = vQ\mathrm{s}$. Thus, (13) yields the following values of k to generate non-zero UMP_x:

$$k \pm vQ\mathrm{s} = \pm 1 \quad \rightarrow \quad k = vQ\mathrm{s} \pm 1 \tag{16}$$

If the tolerances of the stator slots are predominant (case of a perfect rotor), according to (9) ℓ can take any value, so $k \pm \ell = \pm 1$ (13) can always be fulfilled. Hence, knowing that from (5) $k = u(2p)$, these are the values of k that generate non-zero UMP_x:

$$k = u(2p) \tag{17}$$

However, if in a PMSM with tolerances there is a symmetry in those tolerances, the new k and ℓ harmonics do not fulfil the condition $k \pm \ell = \pm 1$ of (13) to have non-zero values of UMP_x. As a conclusion, symmetry in tolerances implies that the magnetic flux density is equilibrated and that the UMP is zero. If tolerances are unbalanced there is a displacement in the magnetic flux density and UMP is generated. It is the same effect as having a geometric eccentricity (static and/or dynamic). So, UMP is created by unbalanced tolerances or by eccentricity, not by "tolerances".

B. With static eccentricity

When the PMSM has a SE, the air gap is not constant in all the turn, and varies with the tangential position θ. In the direction of the minimum air gap the pressure is maximum, and vice versa. According to [25], the air gap with SE can be modelled as in Fig. 4, where $g(\theta)$ given by equation (18) is the air gap between the rotor and the stator, g_0 the ideal air gap between the rotor and the stator, and e the value of the eccentricity.
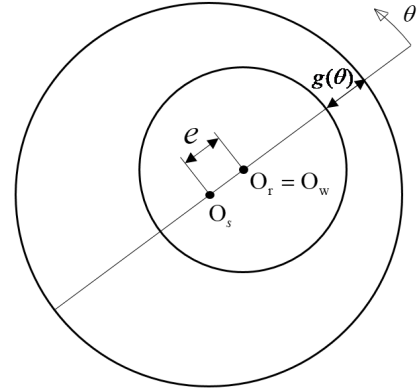

Fig. 4. Air gap with static eccentricity. O_s: Stator symmetry center; O_r: Rotor symmetry center; O_w: Rotor rotation center

$$g(\theta) = g_0 - e\cos\theta \tag{18}$$

To calculate the harmonics generated by the tolerances in the presence of SE, first the air gap of (18) is converted to the dimensionless expression of (19). Then this relative air gap is introduced in (2) to correct the electromagnetic pressure due to SE [15][18] and give the corresponding equation (20).

$$\frac{g(\theta)}{g_0} = 1 - \frac{e}{g_0}\cos\theta \tag{19}$$

$$UMP_x = L_{stk}R_{rot}\int_0^{2\pi} p_r(\theta,t)\frac{g(\theta)}{g_0}\cos\theta\,\mathrm{d}\theta$$

$$UMP_y = L_{stk}R_{rot}\int_0^{2\pi} p_r(\theta,t)\frac{g(\theta)}{g_0}\sin\theta\,\mathrm{d}\theta \tag{20}$$

Introducing (19) in (20) and developing it, an equation for UMP_x is obtained with 12 addends instead of the 4 addends of (11), being the first 4 addends equal to those in (11). Developing this equation similarly as previously done for WE, the result is that, to have non-zero values of UMP_x, any of the conditions of (21) must be fulfilled. This result is obtained from the spatial distribution order of the magnetic pressure. Therefore, the harmonics with SE are the harmonics for the WE case given by $k \pm \ell = \pm 1$, plus the new ones given by $k \pm \ell \pm 1 = \pm 1$.

Spatial orders: $k \pm \ell = \pm 1$
Spatial orders: $k \pm \ell \pm 1 = \pm 1$ (equivalent to $k \pm \ell = \pm 0, \pm 2$) $\tag{21}$

In the case of an ideal PMSM with no tolerances, bearing in mind (5) and (8), a non-zero UMP_x with $k = u(2p)$ harmonics is caused for the k values that agree with condition (22).

$$u(2p) \pm vQ\mathrm{s} = \pm 0, \pm 2 \tag{22}$$

The ±0 condition of (22) is always fulfilled by $k = LCM(Q_s, 2p)$ and its multiples, so the previous result can be expressed in another analogous but more practical way expressing that a non-zero UMP_x will exist with harmonics $k = wLCM(Q_s, 2p)$, plus harmonics $k = u(2p)$ that agree with condition (23):

$$u(2p) \pm vQ_s = \pm 2 \qquad (23)$$

being $w = 0, 1, 2, 3\ldots$ an integer number.

If the tolerances of the magnets are predominant (case of a perfect stator), the stator can be considered perfect and then from (8) the slot harmonics are $\ell = vQ_s$. Hence, (21) yields the following values of k to generate non-zero UMP_x:

$$k = vQ_s \pm 0, 2 \qquad (24)$$

If the tolerances of the stator slots are predominant (case of a perfect rotor), the rotor can be considered perfect and then $k = u(2p)$ from (5). (21) gives the following magnet harmonics:

$$k = u(2p) \qquad (25)$$

C. With dynamic eccentricity

With DE the air gap fluctuates with the tangential position θ and time t. As stated by [25], the air gap can be modelled as in Fig. 5 and (26).
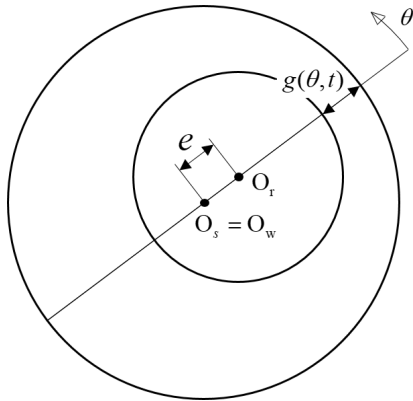

Fig. 5. Air gap with dynamic eccentricity. O_s: Stator symmetry center; O_r: Rotor symmetry center; O_w: Rotor rotation center

$$g(\theta, t) = g_0 - e\cos(\theta - 2\pi f_{rot} t) \qquad (26)$$

As in previous section for SE, first the air gap is converted to the dimensionless expression of (27), and then it is substituted in (2) to update the electromagnetic pressure with the influence of DE. This produces equation (28).

$$\frac{g(\theta, t)}{g_0} = 1 - \frac{e}{g_0}\cos(\theta - 2\pi f_{rot} t) \qquad (27)$$

$$UMP_x = L_{stk} R_{rot} \int_0^{2\pi} p_r(\theta, t) \frac{g(\theta, t)}{g_0} \cos\theta \, d\theta$$

$$UMP_y = L_{stk} R_{rot} \int_0^{2\pi} p_r(\theta, t) \frac{g(\theta, t)}{g_0} \sin\theta \, d\theta \qquad (28)$$

From (28) an equation for UMP_x is obtained again with 12 addends instead of the 4 addends of (11), with the first 4 addends equal to those in (11). To have non-zero values of UMP_x, the results obtained from the spatial distribution order of the magnetic pressure are (21) as in the case of SE. Thus, the conditions in terms of the spatial distribution orders are the same for SE and for DE, but for DE the temporal orders corresponding to the spatial harmonics k are:

$$\text{Temporal orders: } k \pm 1 \qquad (29)$$

Therefore, in SE the harmonics corresponding to the values of k arise, whereas in DE the harmonics corresponding to the values of k±1 arise.

Thus, as a summary, the harmonics with DE are the harmonics for the WE case, plus as in SE the ones given by $k \pm \ell \pm 1 = \pm 1$ from the spatial distribution orders but corrected with a ±1 factor because temporal orders are not equal.

In the case of an ideal PMSM with no tolerances, since $k = u(2p)$ (5), a non-zero UMP_x with $k = u(2p) \pm 1$ harmonics is caused for the k values that agree with condition (22).

$$k = u(2p) \pm 1 \qquad (30)$$

If the tolerances of the magnets are predominant (case of a perfect stator), taking into account that in (8) $\ell = vQ_s$, (21) and (29) yield the following values of k that generate non-zero UMP_x:

$$k = vQ_s \pm 1, 3 \qquad (31)$$

If the tolerances of the stator slots are predominant (case of a perfect rotor), the rotor can be considered perfect and then $k = u(2p)$ from (5). Hence, from (29) the magnet harmonics are (30).

D. Summary of results

The previously calculated mechanical orders generated in the projection of the UMP in a fixed direction for the cases of WE, SE and DE, without or with tolerances (WT, RT, ST or BT) are summarized in Table I, where some of the results are regrouped and simplified. Table II is its equivalent for the magnitude of the UMP, obtained following an analogue process.

TABLE I

MAIN MECHANICAL ORDERS OF THE PROJECTION OF THE UMP WITHOUT ECCENTRICITY, WITH STATIC ECCENTRICITY AND WITH DYNAMIC ECCENTRICITY, DEPENDING ON TOLERANCE TYPE. ANALYTICAL RESULTS

Without eccentricity			
Ideal	Rotor tolerance	Stator tolerance	Rotor + Stator tolerance
$2p \cdot u$ †	$2p \cdot u$ † $Qs \cdot v \pm 1$ *	$2p \cdot u$ † $2p \cdot u$ *	$2p \cdot u$ † $2p \cdot u$ *
Static eccentricity			
Ideal	Rotor tolerance	Stator tolerance	Rotor + Stator tolerance
0 $LCM(Qs, 2p) \cdot w$ $2p \cdot u$ ††	0 $LCM(Qs, 2p) \cdot w$ $2p \cdot u$ †† $Qs \cdot v \pm 1$ * $Qs \cdot v \pm 0,2$	0 $LCM(Qs, 2p) \cdot w$ $2p \cdot u$	0 $LCM(Qs, 2p) \cdot w$ $Qs \cdot v \pm 1$ * $Qs \cdot v \pm 0,2$ $2p \cdot u$
Dynamic eccentricity			
Ideal	Rotor tolerance	Stator tolerance	Rotor + Stator tolerance
1 $LCM(Qs, 2p) \cdot w \pm 1$ $2p \cdot u \pm 1$ ††† $2p \cdot u$ †	1 $LCM(Qs, 2p) \cdot w \pm 1$ $2p \cdot u \pm 1$ ††† $2p \cdot u$ † $Qs \cdot v \pm 1,3$	1 $LCM(Qs, 2p) \cdot w \pm 1$ $2p \cdot u$ † $2p \cdot u$ * $2p \cdot u \pm 1$	1 $LCM(Qs, 2p) \cdot w \pm 1$ $2p \cdot u$ † $Qs \cdot v \pm 1,3$ $2p \cdot u$ * $2p \cdot u \pm 1$

† :   UMP X ≠ 0 only if $2p \cdot u \pm Qs \cdot v = \pm 1$. Not for any u

†† : UMP X ≠ 0 only if $2p \cdot u \pm Qs \cdot v = \pm 1, 2$. Not for any u

††† : UMP X ≠ 0 only if $2p \cdot u \pm Qs \cdot v = \pm 2$. Not for any u

* :   UMP X ≠ 0 only if there is an spatial asymmetry in tolerances

$u = 0,1,2,3...$, $v = 0,1,2,3...$ and $w = 0,1,2,3...$ are integer numbers

LCM = Least Common Multiple

TABLE II

MAIN MECHANICAL ORDERS OF THE MAGNITUDE OF THE UMP WITHOUT ECCENTRICITY, WITH STATIC ECCENTRICITY AND WITH DYNAMIC ECCENTRICITY, DEPENDING ON TOLERANCE TYPE. ANALYTICAL RESULTS

Without eccentricity			
Ideal	Rotor tolerance	Stator tolerance	Rotor + Stator tolerance
	0 $Qs \cdot v$	0 $2p \cdot u$	0 $Qs \cdot v$ $2p \cdot u$
Static eccentricity			
Ideal	Rotor tolerance	Stator tolerance	Rotor + Stator tolerance
0 $LCM(Qs, 2p) \cdot w$ $LCM(Qs, 2p) \cdot w \pm 2p \cdot u$	0 $LCM(Qs, 2p) \cdot w$ $LCM(Qs, 2p) \cdot w \pm 2p \cdot u$ 1 $Qs \cdot v \pm 0,1,2,3...$	0 $LCM(Qs, 2p) \cdot w$ $LCM(Qs, 2p) \cdot w \pm 2p \cdot u$ $2p \cdot u$	0 $LCM(Qs, 2p) \cdot w$ $LCM(Qs, 2p) \cdot w \pm 2p \cdot u$ 1 $Qs \cdot v \pm 0,1,2,3...$ $2p \cdot u$
Dynamic eccentricity			
Ideal	Rotor tolerance	Stator tolerance	Rotor + Stator tolerance
0 $LCM(Qs, 2p) \cdot w$ $LCM(Qs, 2p) \cdot w \pm Qs \cdot v$	0 $LCM(Qs, 2p) \cdot w$ $LCM(Qs, 2p) \cdot w \pm Qs \cdot v$ $Qs \cdot v$	0 $LCM(Qs, 2p) \cdot w$ $LCM(Qs, 2p) \cdot w \pm Qs \cdot v$ 1 $2p \cdot u \pm 0,1,2,3...$	0 $LCM(Qs, 2p) \cdot w$ $LCM(Qs, 2p) \cdot w \pm Qs \cdot v$ $Qs \cdot v$ 1 $2p \cdot u \pm 0,1,2,3...$

$u = 0,1,2,3...$, $v = 0,1,2,3...$ and $w = 0,1,2,3...$ are integer numbers

LCM = Least Common Multiple

III. EXPERIMENTAL MEASUREMENTS OF DIMENSIONS

A. Measurement of the remanent magnetic field of magnets

Before mounting the PMs on the rotor, they were magnetized carefully and their magnetization levels were measured using a magnetic characterizer. The biggest deviation of the magnetization level of one magnet from the mean magnetization level was only 0.26%.

B. Measurement of critical dimensions

The theoretical diameters of the teeth of the stator and the poles of the rotor are known from their drawings. However, dimensions of parts vary according to manufacturing tolerances. Thus, both diameters were measured on the manufactured PMSM and these real dimensions were used later when the geometry of the FE model was built.

1) Measurement of the teeth of the stator:

The stator was positioned on the table of a three-dimensional coordinate measuring machine (CMM) and its inner cylindrical bore formed by the teeth was measured (Fig. 6). The diameter of each one of the $Qs = 36$ teeth was measured in 16 points by a contact probe. Next, the mean of the 16 values was calculated for each tooth and taken as the nominal value of the diameter of the tooth (see these results in Table III). The relative error of Table III was calculated relative to the air gap of 1 mm. Results suggested that deviations of the real diameters of the teeth from the theoretical diameters exceeded values of 5% in most cases and even values of 11% for some teeth. Taking into account that values of eccentricity in the range of 5-10% are considered as residual [4][8][9], the measured values were close or even out of the upper suggested limit.
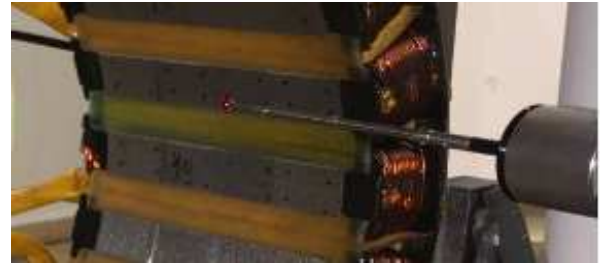

Fig. 6.   Measurement of the teeth of the stator in a three-dimensional coordinate measuring machine

TABLE III

TRUE VALUES OF THE DIAMETERS OF THE TEETH OF THE STATOR: CALCULATIONS BASED ON MEAN VALUES FOR EACH TOOTH (ONLY VALUES OF 1 OUT OF 3 TEETH ARE SHOWN FOR CONCISENESS)

Tooth number	Mean diameter (mm)	Absolute error (mm)	Relative error (%)	
1	221.956	-0.044	-4.41%	
4	222.053	0.053	5.29%	
7	222.093	0.093	9.25%	
10	221.890	-0.110	-10.99%	Minimum diameter
13	222.063	0.063	6.27%	
16	222.114	0.114	11.45%	Maximum diameter
19	221.917	-0.083	-8.32%	
22	222.080	0.080	8.02%	
25	222.104	0.104	10.42%	
28	221.890	-0.110	-10.98%	
31	222.046	0.046	4.55%	
34	222.104	0.104	10.44%	

2) Measurement of the poles of the rotor:

The rotor was positioned on its shaft in the PMSM and its outer cylinder was measured using a dial indicator (Fig. 7). Each of the $2p = 30$ poles was measured in 16 points. Next, the mean of the 16 values was calculated and taken as the nominal deviation of the pole from the theoretical diameter value (see these results in Table IV). Results suggest that deviations of the real diameters of the poles from the theoretical diameters were small, much smaller than for the bore of the stator, and inside the range of 5-10% mentioned beforehand as residual for eccentricity [4][8][9]. In spite of their small value, they were taken into account in the FE model.

Fig. 7. Measurement of the poles of the rotor by means of dial indicators

TABLE IV
TRUE VALUES OF THE DIAMETERS OF THE POLES OF THE ROTOR, MEASURED WITH DIAL INDICATORS: CALCULATIONS BASED ON MEAN VALUES FOR EACH POLE (ONLY VALUES OF 1 OUT OF 3 POLES ARE SHOWN FOR CONCISENESS)

Pole number	Absolute error (mm)	Relative error (%)	
1	0.0087	0.87%	
4	-0.0061	-0.61%	
7	-0.0114	-1.14%	
10	-0.0131	-1.31%	
13	0.0036	0.36%	
16	0.0131	1.31%	
19	-0.0058	-0.58%	
22	-0.0304	-3.04%	Minimum diameter
25	-0.0042	-0.42%	
28	0.0217	2.17%	Maximum diameter

IV. EXPERIMENTAL TEST BENCH

The experimental work is based on the innovative test bench proposed by Galfarsoro et al. in [10]. In this test bench SE is generated mounting the stator on a Kistler type 9255B piezoelectric force sensor and supporting the rotor separately, as done by Chen et al. [7], Lee et al. [11] and Dorrell et al. [12]. The measurement of the three dynamic and quasistatic orthogonal components of the UMP is possible with this decoupling of the stator and the rotor. A second novel mechanism is incorporated into the test bench to create DE, by means of a rotor held by a shaft composed of two eccentric pieces that rotate between them [10]. Previous results showed that the test bench was suitable to generate any value of SE and/or DE in a continuous, fast and controlled way [10]. The multi-channel data acquisition system and BK Connect measurement and analysis software from Brüel & Kjær was used, with 24-bit resolution, anti-aliasing filters and a sampling frequency of 16384 Hz.

In experimental measurements the PMSM under study has certain rotor and stator manufacturing dimensions that cannot be changed. Therefore, the study of manufacturing tolerances was carried out with those original values, and SE and DE were changed.

In the present study the abovementioned test bench was connected to a second EM (Fig. 8). The second EM drove the PMSM under test so that it worked in open circuit. The objective was to avoid the influence of the control on the PMSM under test, since the control could inject harmonics in the current that may later be seen in other measured variables, modifying the effect of the analyzed defects (tolerances and eccentricities).

Regarding control, the second EM was fed by an inverter, which controlled the chosen constant speed. The speed controller was tuned so as to have minimum speed ripple.
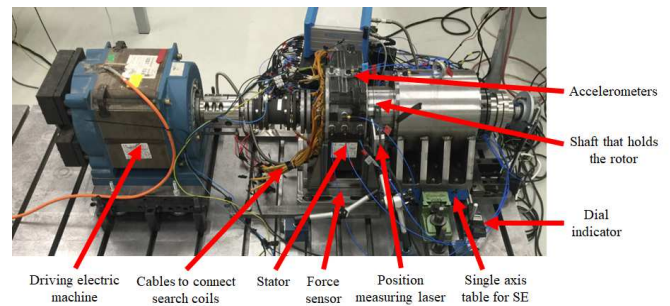

Fig. 8. Experimental test bench for the measurements of the UMP

V. ELECTROMAGNETIC FE SIMULATIONS

A. *Analyzed cases*

Three eccentricity cases were considered in the FE simulations: WE, SE and DE. Within each of these three cases, four kinds of tolerances were simulated implementing the experimentally measured real dimensions: 1) WT (both rotor and stator ideal); 2) RT; 3) ST; 4) BT.

B. *Description of the electromagnetic FE simulations*

With regard to rotor tolerances, in reality there are geometrical tolerances of the steel sheets and of the magnets, and also tolerances of the magnetic properties of the magnets (remanence and magnetic permeability). Not all of them have the same impact on the performance of the machine, but they generate the same harmonics. Thus, for simplicity only the tolerance of the magnetic field remanence was studied, using the experimentally measured value of each magnet. The stator teeth had the experimentally measured real dimensions, hence not all the teeth were equal. The eccentricity grade modeled was 55% of the air gap, and for each simulation the magnitude and the projection of the UMP were calculated.

As the purpose is to assess the manufacturing imperfections, the whole machine had to be drawn since there is no symmetry, as shown in Fig. 9 (top). In order to get a high accuracy in the air gap, it was divided in 3 regions, as it can be seen in Fig. 9 (bottom). Referring to the mesh, the number of nodes was 76245, enough to have a good trade-off between computational load and accuracy.
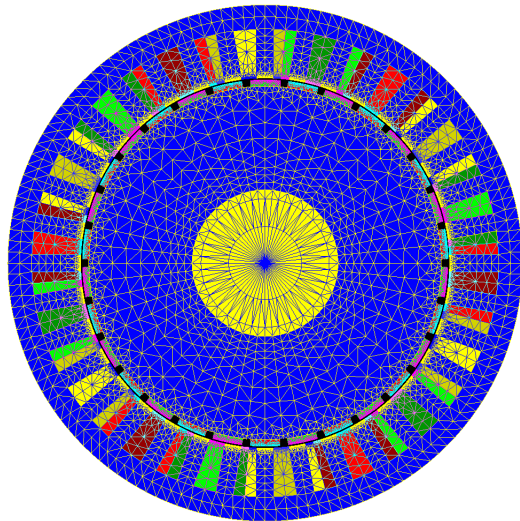
Fig. 9. Meshing: whole model of the PMSM (top); detail of the meshing of the air gap (bottom)

As eccentricity is assessed, there must be two coordinate systems, one for the rotor and another for the stator. For a SE, the movement is around the rotor coordinate system (rotor rotating with regard to its center), and for a DE around the stator one (rotor rotating with regard to the center of the stator).

VI. RESULTS FOR STATIC ECCENTRICITY WITH ORIGINAL TOLERANCES

A. Results of the experimental measurements

The Fast Fourier Transforms (FFTs) of the measured UMPs for increasing values of SE are shown in Fig. 10 (note: all FFTs in this paper are with the abscissa in harmonics of the fundamental electric order). These results confirm that SE changes the frequency content of the UMP, increasing some characteristic orders and decreasing others. Fig. 11 is a zoom of Fig. 10 to highlight two representative electric orders.
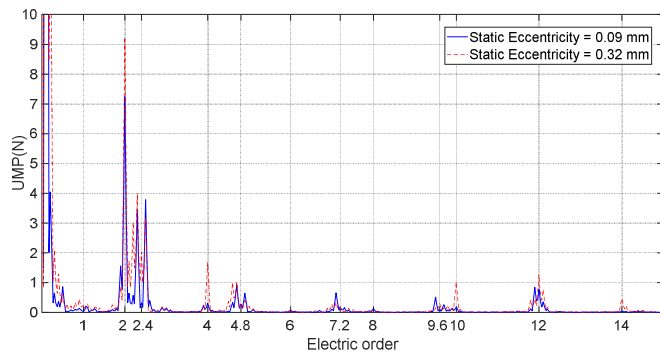
Fig. 10. FFT of the experimental UMP for an increasing value of static eccentricity
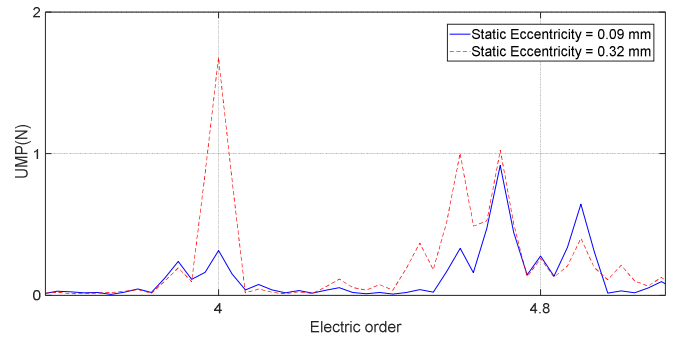
Fig. 11. FFT of the experimental UMP for an increasing value of static eccentricity. Zoom of electric orders 4 and 4.8

B. Results of the electromagnetic FE simulations

Fig. 12 shows the simulated spectra of the UMP, with both rotor and stator real dimensions. Blue peaks of electric orders correspond to the spectrum WE, and red peaks of electric orders to the spectrum with 55% SE. The conclusion is that generally electric orders 2, 4, 6, etc. (multiples of 2) increase without sideband peaks, whilst electric orders 2.4, 4.8, 7.2, etc. (multiples of Qs/p) decrease and their sideband peaks, which are separated $1/p$, increase. Fig. 13 displays two of these electric orders in detail to observe the abovementioned effect.

Fig. 12 takes into account the simultaneous effect of rotor and stator tolerances in the UMP with SE. Alternatively, Fig. 14 and Fig. 15 break down and separate the effect of each of the tolerances on SE. Red peaks of electric orders in Fig. 14 confirm that, if tolerances are disregarded, a SE only generates peaks that are multiples of 2. Comparing green peaks vs. red peaks in Fig. 15, the conclusion is that rotor tolerances generate the increase of electric orders 2.4, 4.8, 7.2, etc. (multiples of Qs/p) and the increase of their sideband peaks that are separated $1/p$. Comparing orange peaks vs. red peaks in Fig. 15, the conclusion is that stator tolerances generate the increase of electric orders 2, 4, 6, etc. (multiples of 2) without sideband peaks. Note: the continuous component (electric order 0) of the UMP in Fig. 14 and Fig. 15 without eccentricity and without tolerances (blue curve) is not 0 because the meshing is not perfectly symmetrical, what produces a tiny numerical error.
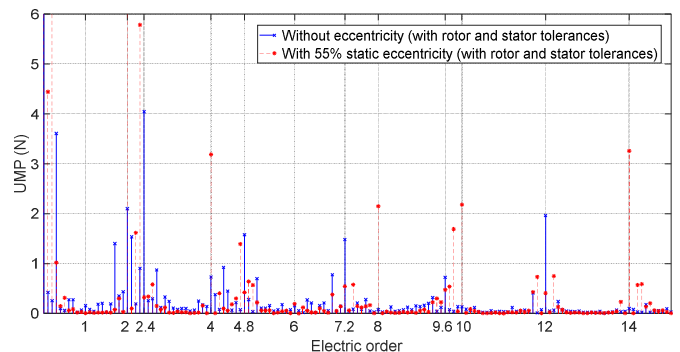

Fig. 12. FFT of the simulated UMP for an increasing value of static eccentricity. Rotor and stator with tolerances
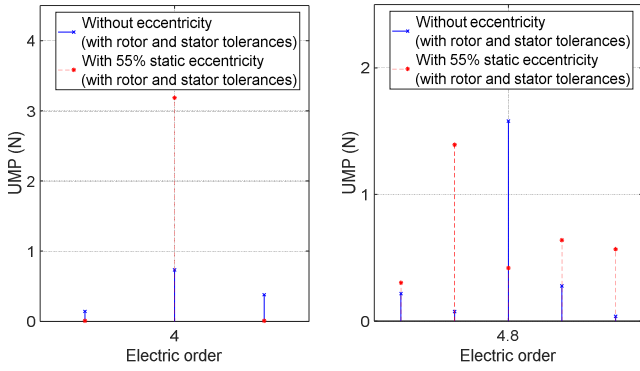
Fig. 13. FFT of the simulated UMP for an increasing value of static eccentricity. Rotor and stator with tolerances. Zoom of electric orders 4 (left) and 4.8 (right)
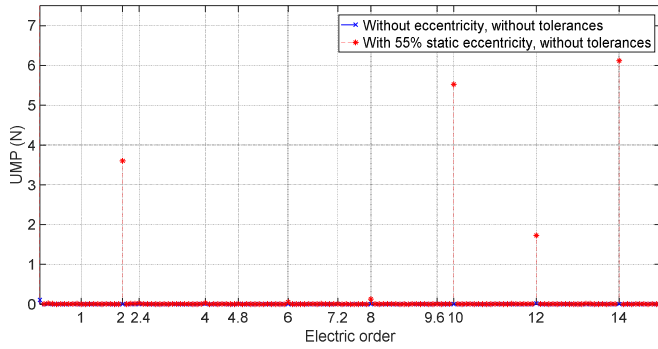

Fig. 14. Effect of static eccentricity on the FFT of the simulated UMP, without tolerances
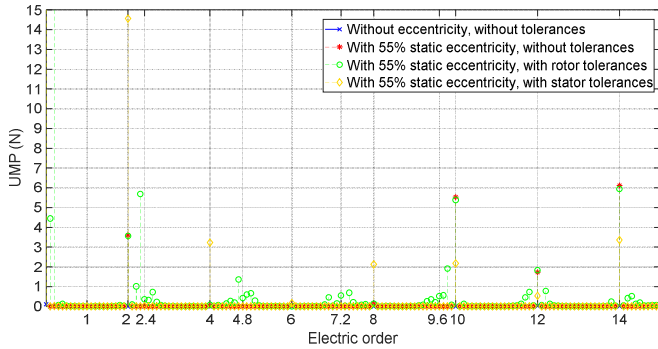

Fig. 15. Effect of tolerances on the FFT of the simulated UMP, with static eccentricity

C. Correlation between experimental and simulation results

Experimental results are only measurable with real manufacturing dimensions on the PMSM under test. Hence, only the cases with both rotor and stator tolerances are going to be compared next.

Regarding SE results, comparison of Fig. 10 for experimental results and Fig. 12 for simulation results produces similar general tendencies in the UMP. That is, a SE generates the increase of electric orders 2, 4, 6, etc. (multiples of 2) without sideband peaks, and variations on the amplitudes of electric orders 2.4, 4.8, 7.2, etc. (multiples of Qs/p) and especially their sideband peaks that are separated $1/p$.

VII.   RESULTS FOR DYNAMIC ECCENTRICITY WITH ORIGINAL TOLERANCES

A. Results of the experimental measurements

The FFTs of the measured UMPs for increasing values of DE are shown in Fig. 16. These results confirm that DE also changes the frequency content of the UMP, increasing some characteristic orders and decreasing others. Fig. 17 is a zoom of Fig. 16 to highlight two representative electric orders.
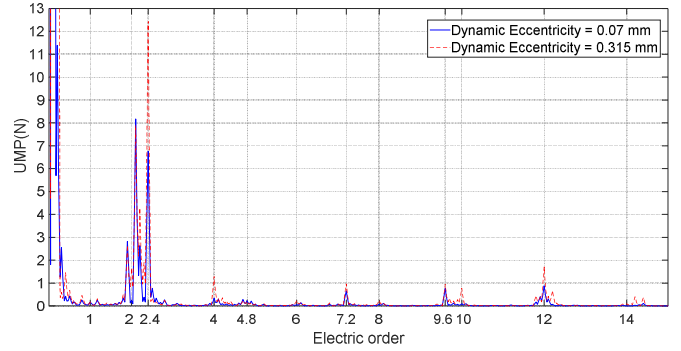

Fig. 16. FFT of the experimental UMP for an increasing value of dynamic eccentricity
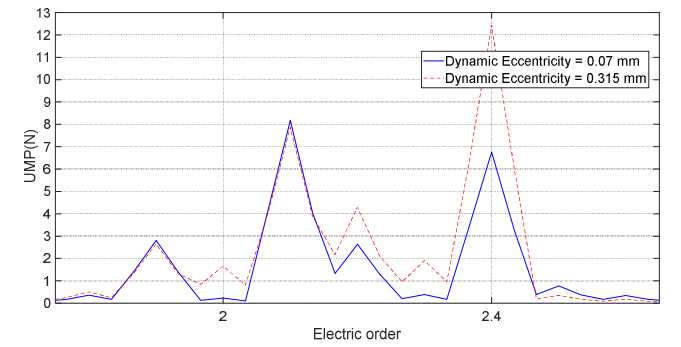

Fig. 17. FFT of the experimental UMP for an increasing value of dynamic eccentricity. Zoom of electric orders 2 and 2.4

B. Results of the electromagnetic FE simulations

Fig. 18 shows the simulated spectra of the UMP with both rotor and stator real dimensions. Blue peaks of electric orders correspond to the spectrum WE, and red peaks of electric orders to the spectrum with 55% DE. The conclusion is that generally electric orders 2, 4, 6, etc. (multiples of 2) increase and their sideband peaks that are separated $1/p$ also increase, whilst electric orders 2.4, 4.8, 7.2, etc. (multiples of Qs/p) increase without sideband peaks. Fig. 19 displays two of these electric orders in detail to observe the abovementioned effect.
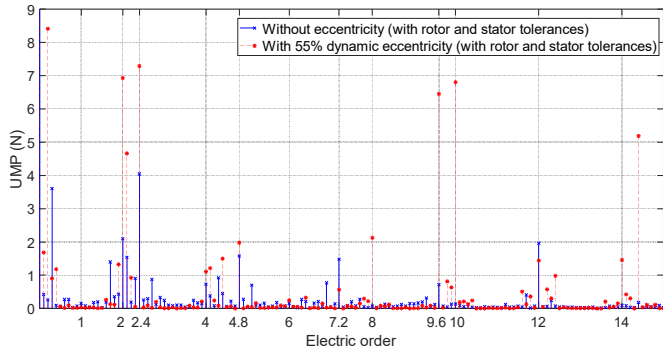
Fig. 18. FFT of the simulated UMP for an increasing value of dynamic eccentricity. Rotor and stator with tolerances
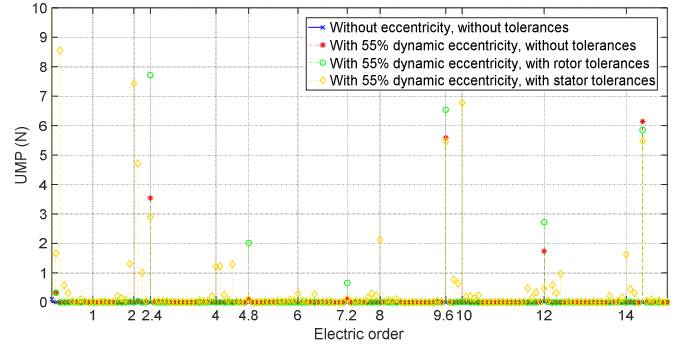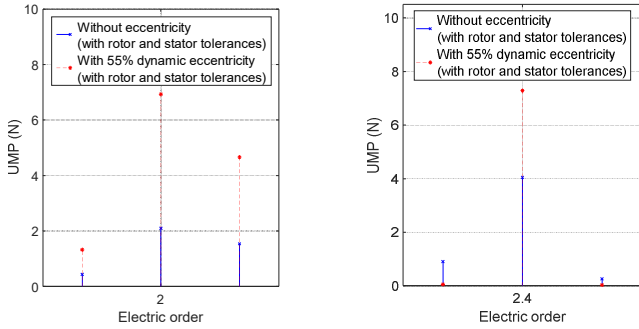

Fig. 19. FFT of the simulated UMP for an increasing value of dynamic eccentricity. Rotor and stator with tolerances. Zoom of electric orders 2 (left) and 2.4 (right)

Fig. 18 takes into account the simultaneous effect of rotor and stator tolerances in the UMP with DE. Alternatively, Fig. 20 and Fig. 21 break down and separate the effect of each of the tolerances on DE. Red peaks of electric orders in Fig. 20 confirm that, if tolerances are disregarded, a DE only generates peaks that are multiples of *Qs/p*. Comparing green peaks vs. red peaks in Fig. 21, the conclusion is that rotor tolerances generate the increase of electric orders 2.4, 4.8, 7.2, etc. (multiples of *Qs/p*) without sideband peaks. Comparing orange peaks vs. red peaks in Fig. 21, the conclusion is that stator tolerances generate the increase of electric orders 2, 4, 6, etc. (multiples of 2) and of their sideband peaks that are separated 1/*p*.
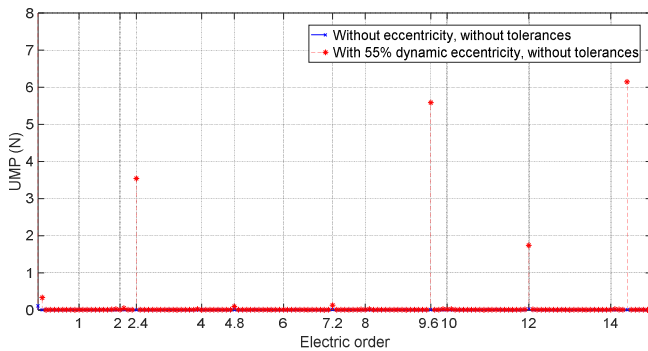

Fig. 20. Effect of dynamic eccentricity on the FFT of the simulated UMP, without tolerances

Fig. 21. Effect of tolerances on the FFT of the simulated UMP, with dynamic eccentricity

The results shown beforehand are based on the magnitude of the UMP. If the projection of the UMP on a fixed direction is considered, results are different for both SE and DE. As an example, Fig. 22 shows the UMP in the fixed horizontal X direction simulated for DE. This figure is the analogous to Fig. 18 but for the UMP in a fixed direction. The interesting remark is that in Fig. 18 electric orders multiples of 2, their 1/*p* separated sideband peaks and electric orders multiples of *Qs/p* are prominent, whilst in Fig. 22 generally electric orders multiples of 2 and *Qs/p* are smaller, 1/*p* separated sideband peaks of multiples of 2 are bigger and multiples of *Qs/p* have new 1/*p* separated sideband peaks. Besides, the biggest electric order for the UMP in the fixed X direction is 1/*p*, instead of order 0 as it occurs for all previous spectra obtained for the magnitudes of the UMP.
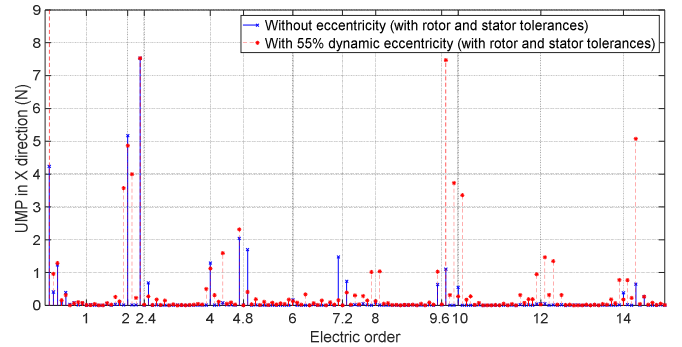

Fig. 22. FFT of the simulated UMP in fixed horizontal X direction for an increasing value of dynamic eccentricity. Rotor and stator with tolerances

C. Correlation between experimental and simulation results

Analyzing DE results, Fig. 16 and Fig. 18 for experimental and simulation results respectively also give similar overall trends in the UMP. Namely, a DE generates the increase of electric orders 2, 4, 6, etc. (multiples of 2) with sideband peaks that are separated 1/*p*, and the increase of electric orders 2.4, 4.8, 7.2, etc. (multiples of *Qs/p*) without sideband peaks.

VIII. CORRELATION OF ANALYTICAL AND FE SIMULATION RESULTS WITH ORIGINAL TOLERANCES

The FE simulation results shown in sections VI and VII for SE and DE respectively confirm the conclusions of the analytical calculations summarized in Table I and Table II. Both analytical and simulation results obtain variations of the same frequency orders with eccentricities and/or tolerances. The conclusion is that SE and DE generate new peaks in the spectra of the magnitude and the projection of the UMP, and that these peaks are dependent on the dimensional tolerances of the rotor and the stator.

IX. ADDITIONAL ANALYSIS WITH INCREASED TOLERANCES OF THE REMANENT MAGNETIZATION LEVELS OF THE MAGNETS

Complementary analysis were carried out with these objectives: 1. Confirm the abovementioned influence of tolerances in the frequency content of the UMP with SE and DE. 2. Analyze if there are orders affected only by tolerances and only by SE and DE, and if so, identify them.

Manufacturing different variants of the machine under test to take into account the effects of tolerances in experimental measurements is time consuming and expensive. In order to limit the resources needed for the process, this study is focused on RT by mounting magnets with different controlled values of their remanent magnetic fields. This is in practice analogous but simpler than mounting sheets of the rotor with different dimensions and placing equal magnets at different radii. Modifying the stator was disregarded because building several stators adds extra uncertainties in the study. Machining the outer diameter of the rotor or the inner diameter of the stator was also omitted because the diameters can only be decreased or increased respectively, and the air gap cannot be kept constant.

Four sets of magnets were magnetized for the experimental measurements with deviations of ±X% with regard to the ideal magnets, being X = 0, 6, 12 and 18. Half of the magnets were magnetized with +X% and the other half with –X%. 0% is the ideal case with all magnets perfectly magnetized, and the other values are big to observe clearly the effect of tolerances. Table V shows the properties of the four sets of magnets. The four sets of magnets were mounted on the rotor analogously, with a certain position for each magnet to assure repeatability. The adopted criterion was to choose the spatial distribution that maximizes the Qs/p electric order in the cogging torque.

FE simulations were also performed with the same configurations defined for experimental measurements.

TABLE V
REMANENT MAGNETIC FIELDS OF THE MAGNETS IN THE FOUR ADDITIONAL MEASUREMENTS WITH INCREASED TOLERANCES

	Magnetization levels of magnets	Mean value of all magnets (T)	Peak to peak of all magnets (% with regard to mean value)	Standard deviation of all magnets (% with regard to mean value)
1	Half of magnets: 1 T Half of magnets: 1 T	1.00	0.06	0.02
2	Half of magnets: 1.06 T Half of magnets: 0.94 T	1.00	12.47	6.27
3	Half of magnets: 1.12 T Half of magnets: 0.88 T	1.00	24.39	12.30
4	Half of magnets: 1.18 T Half of magnets: 0.82 T	1.00	36.39	18.43

X. RESULTS WITH INCREASED TOLERANCES OF THE REMANENT MAGNETIZATION LEVELS OF THE MAGNETS

A. Methodology to detect frequency orders indicators of rotor tolerance

Some electric orders are helpful to identify RT because their amplitudes are independent of eccentricity. These are horizontal and separated lines in the UMP vs. Eccentricity figures. The FE simulation results of Fig. 23, Fig. 24 and Fig. 25 are samples of some of these electric orders. Experimental results, like the examples of Fig. 26 and Fig. 27, confirm the simulation results. However, not all orders show this pattern that allows to detect RT, as revealed by the simulation result of the example of Fig. 28.
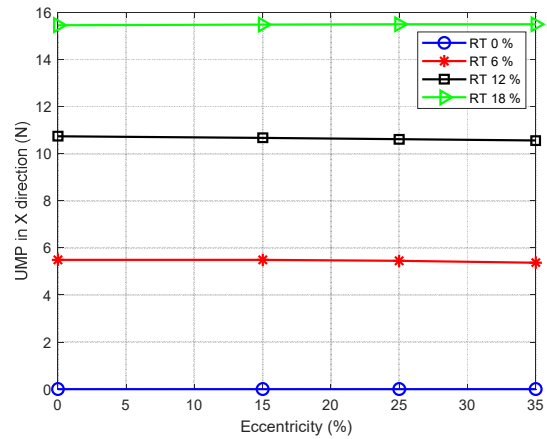

Fig. 23. UMP in fixed horizontal X direction for electric order $(Qs-1)/p$, for an increasing value of static eccentricity and various rotor tolerances. FE simulation result
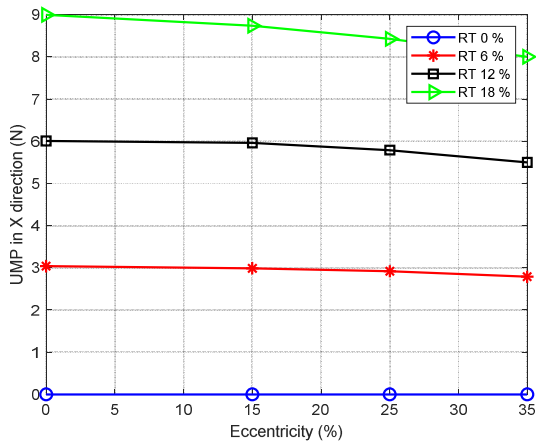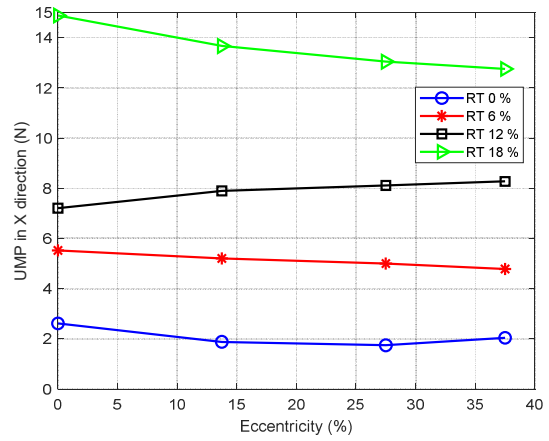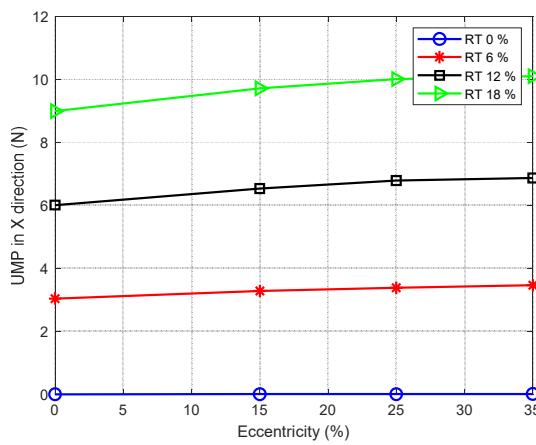
Fig. 24. UMP in fixed horizontal X direction for electric order (2*Qs*+1)/*p*, for an increasing value of static eccentricity and various rotor tolerances. FE simulation result

Fig. 25. UMP in fixed horizontal X direction for electric order (2*Qs*+1)/*p*, for an increasing value of dynamic eccentricity and various rotor tolerances. FE simulation result
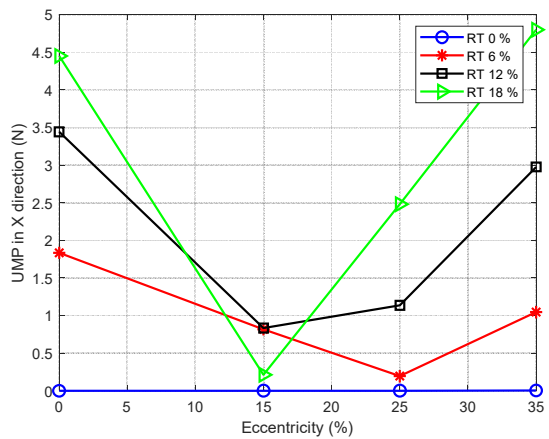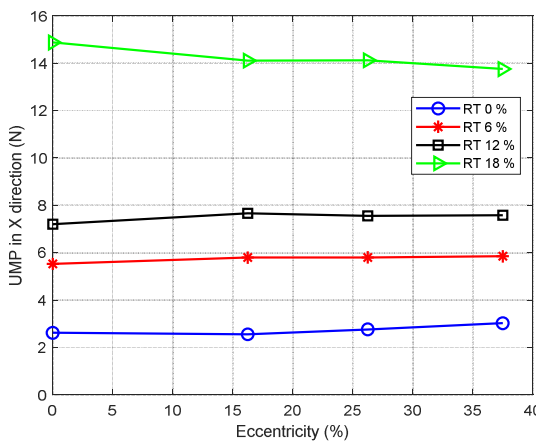

Fig. 26. UMP in fixed horizontal X direction for electric order (2*Qs*+1)/*p*, for an increasing value of static eccentricity and various rotor tolerances. Experimental result at 7.2 r/min

Fig. 27. UMP in fixed horizontal X direction for electric order (2*Qs*+1)/*p*, for an increasing value of dynamic eccentricity and various rotor tolerances. Experimental result at 7.2 r/min

Fig. 28. UMP in fixed horizontal X direction for electric order (*Qs*+1)/*p*, for an increasing value of dynamic eccentricity and various rotor tolerances. FE simulation result

The mechanical orders that are suitable to assess RT with the projection of UMP agree with the values of $k \cdot Q\text{s} \pm 1$ (being $k = 1, 2, 3 \ldots$). Another conclusion is that the projection of UMP gives better results than the magnitude of the UMP.

The abovementioned experimental results were obtained with the PMSM of the test bench driven by a second EM, as explained in section *IV. Experimental test bench*. However, additional measurements with the PMSM rotating autonomously by itself produced similar experimental results, as shown in Fig. 29 and Fig. 30.
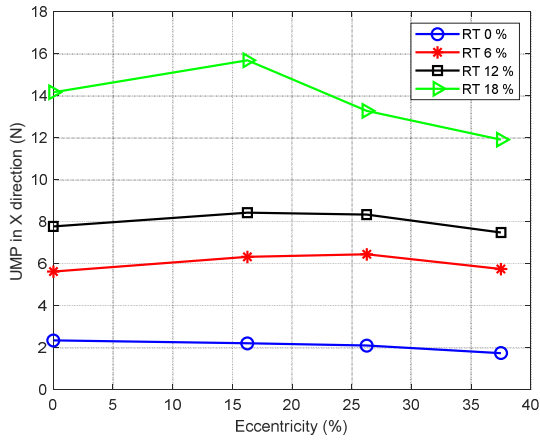
Fig. 29. UMP in fixed horizontal X direction for electric order $(2Qs+1)/p$, for an increasing value of static eccentricity and various rotor tolerances. Experimental result at 7.2 r/min, with PMSM rotating autonomously
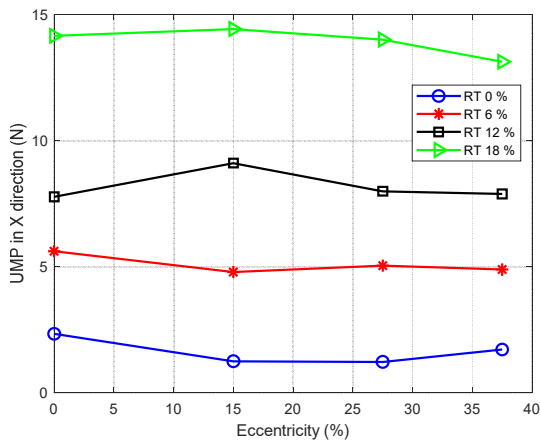

Fig. 30. UMP in fixed horizontal X direction for electric order $(2Qs+1)/p$, for an increasing value of dynamic eccentricity and various rotor tolerances. Experimental result at 7.2 r/min, with PMSM rotating autonomously

B. Methodology to detect frequency orders indicators of eccentricity

Some orders vary only with RT, as explained previously. However, most orders vary with both tolerances and eccentricities. To identify orders that are independent of RT and depend only on eccentricities, and are therefore indicators of such a fault, a new method based on two adjacent orders is proposed. For UMP in a fixed direction, the ratio of amplitudes of electric orders $(Qs-1)/p$ and Qs/p (the ratio of the data of Fig. 23 and Fig. 31) is calculated. Fig. 32 shows this ratio. The data of Fig. 23 allows estimating the level of RT, and once this is known, from the information of Fig. 31 the level of SE can be calculated because RT and SE are decoupled. The requirements for the success of this method are that the lines of the ratios of amplitudes must be approximately horizontal (so that RT does not influence) and well separated (so that different SE values can be differentiated). The results of the example of Fig. 32 fulfill these two conditions. The ideal cases of RT and SE values equal to zero are not shown in Fig. 32 because in those cases Qs/p harmonics should not exist and that leads to values of the ratio that have no sense. In reality, all PMSMs have a certain amount of RT and eccentricity due to fabrication

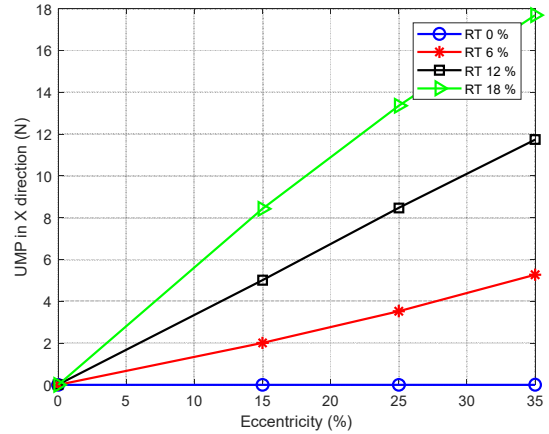tolerances, so this does not occur and the method is effective.

Fig. 31. UMP in fixed horizontal X direction for electric order Qs/p, for an increasing value of static eccentricity and various rotor tolerances. FE simulation result
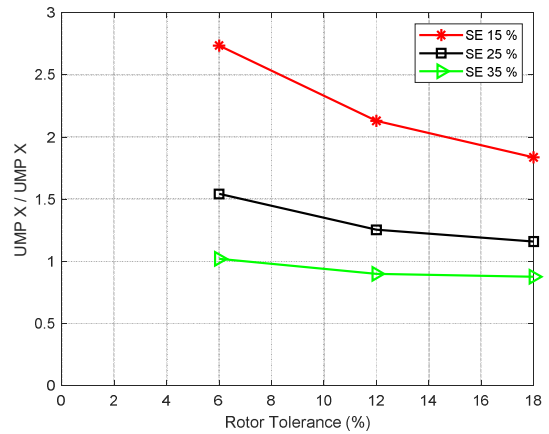

Fig. 32. Ratio of amplitudes of UMP in fixed horizontal X direction for electric orders $(Qs-1)/p$ and Qs/p, for an increasing value of static eccentricity and various rotor tolerances. FE simulation result

The experimental result of Fig. 33, obtained for the same ratio of amplitudes of the projection of the UMP of electric orders $(Qs-1)/p$ and Qs/p, agrees with the simulation results. In both results the bigger the SE the smaller the ratio is, being its slope negative in general. As explained in section III, for the experimental measurements in the test bench the PMs were magnetized carefully with very small deviations of the magnetization levels with regard to the mean value. However, for the nominal value of 0% RT, the RT is not exactly 0% because there are always minor deviations during the magnetization process. This residual RT values make the difference with the FE simulation process, where 0% RT is exact. Fig. 34 is a similar example for DE.
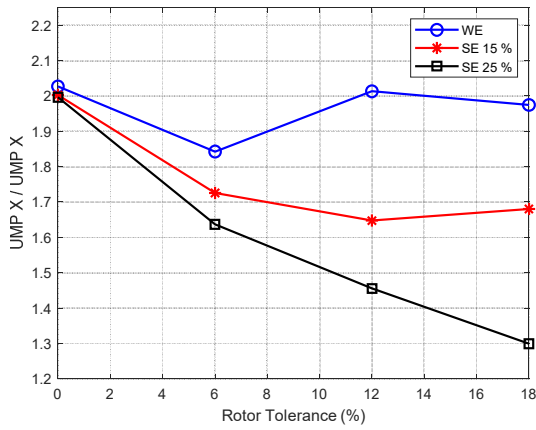
Fig. 33. Ratio of amplitudes of UMP in fixed horizontal X direction for electric orders $(Qs\text{-}1)/p$ and Qs/p, for an increasing value of static eccentricity and various rotor tolerances. Experimental result at 7.2 r/min
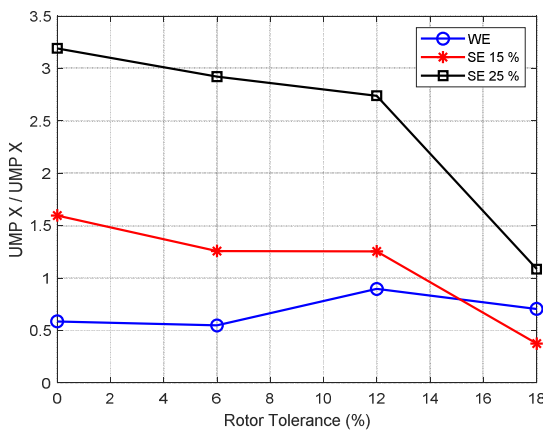

Fig. 34. Ratio of amplitudes of UMP in fixed horizontal X direction for electric orders $(4p+1)/p$ and $4p/p$, for an increasing value of dynamic eccentricity and various rotor tolerances. Experimental result at 96 r/min

The conclusion is that with the projection of UMP, the ratios of the amplitudes of mechanical orders $k \cdot Qs$ with their sidebands identify SE, and the ratios of the amplitudes of mechanical orders $k \cdot 2p$ with their sidebands indicate DE (being $k = 1, 2, 3 \ldots$). The projection of UMP gives again better results than the magnitude of the UMP.

XI. CONCLUSIONS

The UMP of a PMSM was measured experimentally, and calculated analytically and by FE simulation, with similar trends in results. The main conclusion is that the frequency components of the UMP with eccentricity depend not only on the type and level of eccentricity, but also on the tolerances of the dimensions of the rotor and the stator (and presumably on the tolerances of other dimensions of the parts of the motor and on the tolerances of the magnetization levels of the magnets). Furthermore, the influence of the tolerances is significant, since some of the biggest peaks in the FFT of the UMP only exist if the tolerances are present.

Table I and Table II summarize the frequency orders generated in all eccentricity and tolerance combinations for the projection and the magnitude of the UMP.

In the design phase of an electric motor, the approach is to simulate the UMP considering both eccentricities and tolerances, to know the influence of each of them. This gives the possibility to select the specific eccentricities or tolerances with biggest influence on the high amplitude orders of the UMP and act on them, reducing their amplitudes. In the end, the only solution is to improve the manufacturing processes to decrease the selected tolerances and consequently maybe also the eccentricities. In other words, with tolerances many harmonic orders arise, which are not generated in ideal healthy electric machines. Thus, the only method to improve them is to decrease tolerances.

The amplitudes of the UMP harmonics are subjected to the manufacturing tolerances, so they change from one motor unit to another. Therefore, a robust eccentricity detection procedure must consider this. Otherwise, erroneous eccentricity estimations can be given and harmonics originated by tolerances and by eccentricities can be misidentified.

Frequency orders of the UMP that are independent from eccentricities and are hence indicators of rotor tolerances are calculated (see Table VI). Besides, an additional novel method based on the ratio of amplitudes of the UMP of two adjacent spectral orders is proposed to identify orders that are independent from rotor tolerances and depend only on eccentricities, and are therefore indicators of such a fault (see Table VI). Well-correlated FE simulation and experimental measurements validate these results. A last conclusion is that the projection of UMP in a fixed direction gives better results than the magnitude of the UMP to identify tolerance and eccentricity errors.

TABLE VI
SUMMARY: MECHANICAL ORDERS THAT ARE INDICATORS OF ROTOR TOLERANCE, AND RATIOS OF MECHANICAL ORDERS THAT ARE INDICATORS OF ECCENTRICITIES

Rotor Tolerance indicators	
UMP X SE	UMP X DE
$Qs \cdot k \pm 1$	

Eccentricity indicators	
UMP X SE	UMP X DE
$\dfrac{Qs \cdot k \pm 1}{Qs \cdot k}$	$\dfrac{2p \cdot k \pm 1}{2p \cdot k}$

As future line, a further research is underway to investigate the capability of the developed methodology with other signals such as current, voltage and vibrations, to facilitate its applicability.

XII. APPENDIX

TABLE VII
PMSM UNDER TEST MAIN SPECIFICATIONS

Pole pairs (p)	15
Number of slots of the stator (Qs)	36
Rotor outer diameter / length	220 mm / 100 mm
Stator inner diameter / length	222 mm / 100 mm
Air gap	1 mm
Rated speed	96 r/min

XIII. ACKNOWLEDGMENT

XIV. REFERENCES

[1] U. Galfarsoro, A. McCloskey, S. Zarate, X. Hernández, and G. Almandoz, "Influence of manufacturing tolerances and eccentricities on the unbalanced magnetic pull in permanent magnet synchronous motors," in *2020 XIII International Conference on Electrical Machines (ICEM)*, 2020.

[2] M. Yilmaz, "Limitations/capabilities of electric machine technologies and modeling approaches for electric motor design and analysis in plug-in electric vehicle applications," *Renewable and Sustainable Energy Reviews*, vol. 52, pp. 80–99, 2015.

[3] J. R. Riba, C. López-Torres, L. Romeral, and A. Garcia, "Rare-earth-free propulsion motors for electric vehicles: A technology review," *Renewable and Sustainable Energy Reviews*, vol. 57, pp. 367–379, May 2016.

[4] J. Hong, S. Park, D. Hyun, T. Kang, S. B. Lee, C. Kral, and A. Haumer, "Detection and classification of rotor demagnetization and eccentricity faults for PM synchronous motors," *IEEE Transactions on Industry Applications*, vol. 48, no. 3, pp. 923–932, May 2012.

[5] *VDI 3839-5:2001. Instructions on measuring and interpreting the vibration of machines - Typical vibration patterns with electrical machines*. VDI (The Association of German Engineers), 2001.

[6] W. le Roux, R. G. Harley, and T. G. Habetler, "Detecting Rotor Faults in Low Power Permanent Magnet Synchronous Machines," *IEEE Transactions on Power Electronics*, vol. 22, pp. 322–328, Jan. 2007.

[7] X. Chen, Z. Deng, J. Hu, and T. Deng, "An analytical model of unbalanced magnetic pull for PMSM used in electric vehicle: Numerical and experimental validation," *International Journal of Applied Electromagnetics and Mechanics*, vol. 54, no. 4, pp. 583–596, 2017.

[8] S. Nandi, H. A. Toliyat, and X. Li, "Condition Monitoring and Fault Diagnosis of Electrical Motors - A Review," *IEEE Transactions on Energy Conversion*, vol. 20, pp. 719–729, Dec. 2005.

[9] B. M. Ebrahimi, M. J. Roshtkhari, J. Faiz, and S. V. Khatami, "Advanced eccentricity fault recognition in permanent magnet synchronous motors using stator current signature analysis," *IEEE Transactions on Industrial Electronics*, vol. 61, no. 4, pp. 2041–2052, Apr. 2014.

[10] U. Galfarsoro, A. McCloskey, X. Hernandez, G. Almandoz, S. Zarate, and X. Arrasate, "Eccentricity detection procedure in electric motors by force transducer and search coils in a novel experimental test bench," in *12th IEEE International Symposium on Diagnostics for Electrical Machines, Power Electronics and Drives (SDEMPED 2019)*, 2019, pp. 220–226.

[11] C. I. Lee and G. H. Jang, "Experimental measurement and simulated verification of the unbalanced magnetic force in brushless DC motors," *IEEE Transactions on Magnetics*, vol. 44, no. 11, pp. 4377–4380, 2008.

[12] D. Dorrell and A. Smith, "Calculation and measurement of unbalanced magnetic pull in cage induction motors with eccentric rotors. II. Experimental investigation," *IEE Proceedings-Electric Power Applications*, vol. 143, no. 3, pp. 202–210, 1996.

[13] G. Bramerdorfer, "Tolerance Analysis for Electric Machine Design Optimization: Classification, Modeling and Evaluation, and Example," *IEEE Transactions on Magnetics*, vol. 55, no. 8, pp. 1–9, 2019.

[14] N. Taran, V. Rallabandi, D. M. Ionel, P. Zhou, M. Thiele, and G. Heins, "A systematic study on the effects of dimensional and materials tolerances on permanent magnet synchronous machines based on the IEEE Std 1812," *IEEE Transactions on Industry Applications*, vol. 55, no. 2, pp. 1360–1371, 2018.

[15] A. Mccloskey Gómez, "Prediction of noise and vibration of electromagnetic origin in electrical machines," Mondragon Unibertsitatea, PhD thesis, 2016.

[16] D. Guo, F. Chu, and D. Chen, "The unbalanced magnetic pull and its effects on vibration in a three-phase generator with eccentric rotor," *Journal of sound and Vibration*, vol. 254, no. 2, pp. 297–312, 2002.

[17] T. P. Holopainen, A. Tenhunen, E. Lantto, and A. Arkkio, "Unbalanced magnetic pull induced by arbitrary eccentric motion of cage rotor in transient operation. Part 2: Verification and numerical parameter estimation," *Electrical Engineering*, vol. 88, no. 1, pp. 25–34, 2005.

[18] I. Gómez, G. Almandoz, J. Poza, G. Ugalde, and A. J. Escalada, "Analytical model to calculate radial forces in permanent-magnet synchronous machines," in *2014 International Conference on Electrical Machines (ICEM)*, 2014, pp. 2681–2687.

[19] M. Mair, B. Weilharter, and K. Ellermann, "Rotor vibrations in electrical machines due to electromagnetic forces," in *Proceedings of the 9th IFToMM International Conference on Rotor Dynamics*, 2015, pp. 601–611.

[20] P. Pennacchi, "Computational model for calculating the dynamical behaviour of generators caused by unbalanced magnetic pull and experimental validation," *Journal of Sound and Vibration*, vol. 312, no. 1, pp. 332–353, 2008.

[21] Y. Yu, C. Bi, P. N. Hla, Q. Jiang, S. Lin, N. L. H. Aung, and A. Al Mamun, "Incline unbalanced magnetic pull induced by misalignment rotor in PMSM," *IEEE transactions on magnetics*, vol. 49, no. 6, pp. 2709–2714, 2013.

[22] L. Wu, Z. Zhu, J. Chen, and Z. Xia, "An analytical model of unbalanced magnetic force in fractional-slot surface-mounted permanent magnet machines," *IEEE Transactions on Magnetics*, vol. 46, no. 7, pp. 2686–2700, 2010.

[23] Z. Q. Zhu, D. Ishak, D. Howe, and J. Chen, "Unbalanced magnetic forces in permanent-magnet brushless machines with diametrically asymmetric phase windings," *IEEE Transactions on Industry Applications*, vol. 43, no. 6, pp. 1544–1553, 2007.

[24] M. Huo, S. Wang, J. Xiu, and S. Cao, "Effect of magnet/slot combination on triple-frequency magnetic force and vibration of permanent magnet motors," *Journal of Sound and Vibration*, vol. 332, no. 22, pp. 5965–5980, 2013.

[25] L. Cappelli, Y. Coia, F. Marignetti, and Z. Q. Zhu, "Analysis of eccentricity in permanent-magnet tubular machines," *IEEE Transactions on Industrial Electronics*, vol. 61, no. 5, pp. 2208–2216, 2013.